Physica Scripta. Vol. 56, 14–19, 1997

The Method of Phase Retrieval of Complex Wavefield from Two Intensity Measurements Applicable to Hard X-rays

Victor G. Kohn

Russian Research Centre "Kurchatov Institute," 123182, Moscow, Russia

Received September 28, 1996; accepted October 21, 1996

Abstract

A novel algorithm for a reconstruction of the phase shift profile produced by a transparent object in a coherent wave, from a set of two recorded intensity distributions is presented. Contrary to well known algorithms of in-line holography, the method works under the near-field condition where the size of the first Fresnel zone is much less than the characteristic size of the object's details. Such a condition is typical for an in-line holography experimental setup with the use of coherent high energy X-rays ($E > 20$ keV) produced by synchrotron radiation sources of the third generation like ESRF. The novel algorithm is fast and insensitive to a partial loss of coherence or weak detector resolution. The method can be applied to X-ray refraction tomography.

1. Introduction

As it is well known, transparent objects produce only a phase shift of the light wave passing through them. This perturbation cannot be measured directly by a detector which feels only an intensity variation. If the object is illuminated by a coherent wave then the inhomogeneous phase shift transforms to an inhomogeneous distribution of intensity in space at some distance from the object. This fringe pattern accumulates the information about the phase shift profile and can be called in-line hologram similarly to the well known technique for opaque particles [1–3]. The method of reconstruction of the phase shift from the hologram has to be developed for practical use of in-line holography. In standard Gabor in-line holography the image arises in space at the same distance from the hologram as in recording when it is illuminated by the same coherent wave (a plane wave, for example). Such a technique of reconstruction is not possible for a phase object because the phase of the wavefield is invisible. Therefore, computer methods of recovering the phase from an inhomogeneous intensity have to be applied.

A lot of different algorithms have been proposed in recent time for a solution of this task in the case of complex-valued objects which produce refraction and absorption of the radiation simultaneously (see, for example, [4–7]). The task can be formulated in this case as a phase retrieval from two intensity measurements at two planes separated by a definite distance. From the point of view of Fresnel diffraction we should distinguish between the far-field condition and the near-field condition. Only the far-field condition, when the size of the first Fresnel zone is comparable with the size of object, is acceptable for these algorithms. In addition, the wave scattered by the object must be much smaller than the incident wave. These conditions are easy to fulfil in the case of laser illumination of relatively small objects.

Recently, the possibility of imaging the transparent object with coherent high energy X-rays produced by a synchrotron radiation source of the third generation like ESRF has been discovered [8] in the experimental setup of in-line holography. This fact opens the possibility of hard X-ray tomography [9] based on a refraction effect which is much more sensitive in the hard X-ray domain of electromagnetic radiation as compared with the widely used absorption tomography. However, owing to the extremely small wavelengths it is very difficult or impossible to fulfil the far-field condition in the in-line holography experimental setup. Instead, near-field or intermediate conditions are typical. Among the known algorithms of phase retrieval from two intensity measurements only a modified Gerchberg-Saxton iterative algorithm [10, 11] seems to be free from the far-field and small scattering conditions. The technique consists of simulating the direct and back propagations of the wavefield from one plane of measuring to another plane with the use of a propagator function. Starting with an arbitrary phase profile the computer program keeps the calculated phase profile while it replaces the modulus of wavefields by the true known value at each step of iteration. The initial Gerchberg-Saxton algorithm is based on Fourier transformation which is valid in Fraunhofer (far-field) diffraction. Nevertheless, the same procedure works for any other propagator function.

As it is known, this method requires a large number of iterations. Moreover, the convergence is not guaranteed in the general case. Our computer application of this method for hard X-ray in-line holography shows that it works under far-field and intermediate conditions but does not work under the near-field condition which only exists with extremely high-energy X-rays ($E > 40$ keV). Another difficulty of using this method under the near-field condition is that the propagator becomes a very high frequency oscillating function and the use of a Fast Fourier Transformation procedure cannot give the necessary accuracy.

Thus, the possibility of refraction tomography with hard X-rays depends on the successful solution of the problem of phase shift reconstruction under the near-field condition. No approach applicable to laser light illumination can be used and it is necessary to find a quite novel way of solution. In the present paper I propose an approach which is based on ideas of geometrical optics. As it is known, geometrical optics work just under the near-field condition, namely, at small distances and short wavelengths when the wavelength of radiation is much smaller than the characteristic size of the object.

In the next Section a general formulation of the problem is given. Here I consider only a one-dimensional object which has a variable structure only in one direction in a plane perpendicular to the direction of the incident plane wave (a fiber, for example, see Fig. 1). The properties of the

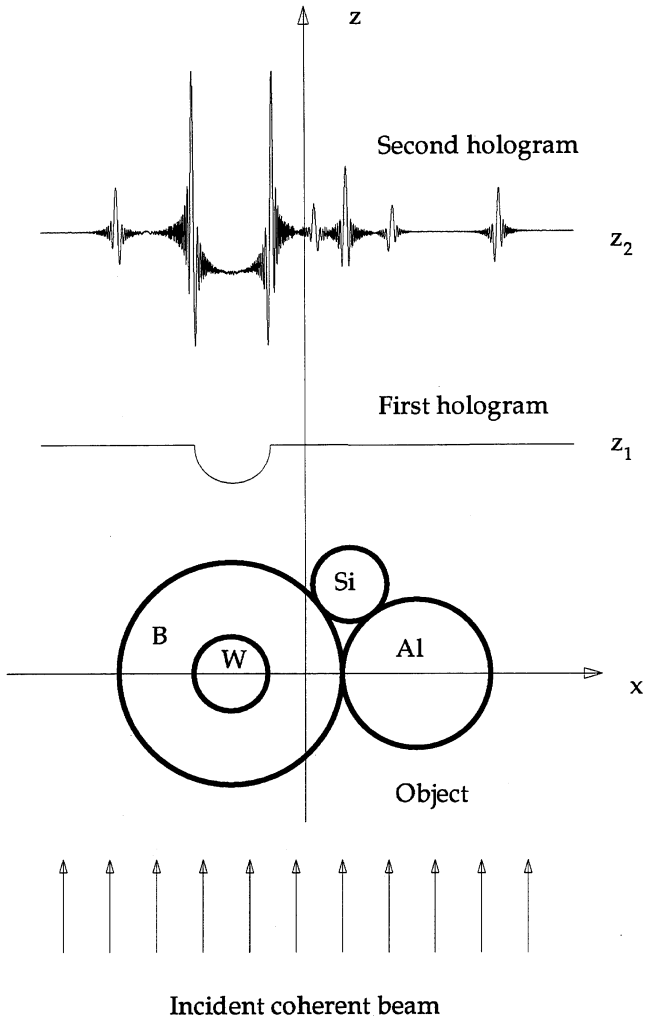

Fig. 1. A scheme of experiment and coordinate system.

propagator function together with standard reconstruction techniques are also analyzed. In Section 3 a novel algorithm is formulated. The algorithm is based on an approximate analytical calculation of the convolution integral. As a result, a differential nonlinear equation has been found which allows to calculate the phase shift profile from the known difference between the recorded intensity distributions at two distances. The algorithm is much faster than the Gerchberg-Saxton algorithm. It is of interest that the partial loss of spatial coherence owing to the finite size of the source and a finite detector resolution does not lead to a loss of information about the phase shift profile. Moreover, the characteristic smoothing of recorded fringe patterns is necessary to avoid the influence of interference between different rays at the same point. A typical example of the applicability of the technique proposed is demonstrated in the last Section.

2. Standard object reconstruction algorithms

Let us consider a simple experimental setup of in-line holography (Fig. 1). The object is homogeneous along the Y-axis and has finite sizes in the X–Z plane. It is illuminated by a plane wave with a unit amplitude $\exp(2\pi iz/\lambda)$ (coherent beam of radiation) moving in the positive z-direction. Here λ is the wavelength. Thanks to the refraction and the absorption of the radiation by the object and the subsequent diffraction of the perturbed wavefield, the homogeneous distribution of the plane wave transforms to complex-valued functions of x, namely $f_1(x)$ and $f_2(x)$ at the positions z_1 and z_2. The holograms record the intensity as the square modulus of the complex wavefield

$$H_1(x) = |f_1(x)|^2, \qquad H_2(x) = |f_2(x)|^2 \tag{1}$$

while the wavefields themselves are connected in accordance with the Fresnel-Kirhhoff principle [12] by means of convolution with the propagator function

$$f_2(x) = \int \mathrm{d}x_1 P_z(x - x_1) f_1(x_1) = P_z(x - x_1) * f_1(x_1). \tag{2}$$

Here and below the sign $*$ means a convolution as an integral over the variable appearing twice. In a usual approximation when the transversal dimension of the holographic images are much smaller than the distance z between them we can use a small angle approximation of the spherical wave and omit the terms in phases connected with a longitudinal movement. Then the propagator for a one-dimensional case can be written as follows

$$P_z(x) = (\mathrm{i}\lambda z)^{-1/2} \exp\left(\mathrm{i}\pi \frac{x^2}{\lambda z}\right) \tag{3}$$

where $z = z_2 - z_1$ is the distance between the holograms. Hereby, the problem is to calculate the phases of the wavefields $f_1(x)$ and $f_2(x)$ from two intensity distributions (1) by means of connection (2) with a propagator function (3).

Taking into account the known expression of the Fourier image of the propagator

$$p_z(q) = \int \mathrm{d}x \exp(-\mathrm{i}qx) P_z(x) = \exp\left(-\mathrm{i}\frac{\lambda z}{4\pi} q^2\right) \tag{4}$$

and the known property of the convolution one can easily verify the following properties of the propagator (3)

$$\begin{aligned}
&P_{z_1}(x - x_1) * P_{z_2}(x_1 - x_2) = P_{z_1 + z_2}(x - x_2),\\
&P_{z_1}(x - x_1) * P^*_{z_2}(x_1 - x_2) = P_{z_1 - z_2}(x - x_2),\\
&P_z(x - x_1) * 1(x_1) = 1(x),\\
&P_0(x - x_1) = \delta(x - x_1).
\end{aligned} \tag{5}$$

Here $1(x)$ means the constant function which equals unity for all x, while $\delta(x)$ is a standard Dirac delta-function which equals infinity for zero argument and zero for all other values of argument.

These properties allow to express the hologram $H_2(x)$ in terms of the object function $o_1(x) = f_1(x) - 1$ as follows

$$\begin{aligned}
H_2(x_1) = 1 &+ P_z(x_1 - x) * o_1(x)\\
&+ P^*_z(x_1 - x) * o^*_1(x)\\
&+ |P_z(x_1 - x) * o_1(x)|^2.
\end{aligned} \tag{6}$$

A standard computed reconstruction technique (see, for example, [3–6]) corresponds to the optical reconstruction setup, namely, illustrating the hologram itself to obtain the object at the same distance. It considers the function

$$\begin{aligned}
R_0(x) &= P^*_z(x - x_1) * [H_2(x_1) - 1]\\
&= o_1(x) + P^*_{2z}(x - x_1) * o^*_1(x_1)\\
&\quad + P^*_z(x - x_1) * |P_z(x_1 - x_2) * o_1(x_2)|^2.
\end{aligned} \tag{7}$$

This function contains three terms which are called an object, a twin-image and an intermodulation term. Under the far-field condition (Fraunhofer diffraction) when $\lambda z \gg d^2$ where d is the characteristic size of the object function, one obtains the focused image, the defocused twin-image and smoothed small intermodulation term as a background.

However, even in this case the function $R_0(x)$ is not an object function in an integral sense because of a pure transparent object

$$\int dx R_0(x) = 1(x) * P_z^*(x - x_1) * [H_2(x_1) - 1]$$

$$= \int dx_1 [H_2(x_1) - 1] = 0. \tag{8}$$

The last relation shows simply that the transparent object cannot change the integral intensity. Such a relation is absent for an object function itself. Therefore the standard reconstruction technique is based on focusing the object image with simultaneous defocusing of all other parts of the function. When the far-field condition is not met eq. (7) becomes a particular form of integral equation for calculating the object function by means of numerical iterative methods. However, under the near-field condition of small z the propagator $P_z(x) \approx \delta(x)$ and all three terms of (7) become focused. In this case the integral equation in unacceptable for a computer calculation.

The modified Gerchberg-Saxton algorithm considers direct and back propagations of the wavefield from one to another

$$o_2(x_1) = P_z(x_1 - x) * o_1(x),$$
$$o_1(x) = P_z^*(x - x_1) * o_2(x_1) \tag{9}$$

where

$$o_n(x) = f_n(x) - 1.$$

It is possible to formulate an iterative process which supposes the calculation of o_2 from o_1, then o_1 from o_2 and so on. Starting with an arbitrary phase profile (for example, zero) for $f_1(x)$ one can replace the modulus of the complex functions by the measured value at each step. The properties of this process can be studied only by computer experiments because the analytical theory is absent. The practice shows that this process converges successfully in the cases when the object covers a limited number of Fresnel zones and the outer part of the image recorded is comparable in size with the object shadow. Under the near-field condition this algorithm does not work.

3. Novel approach to a phase retrieval problem under the near-field condition

Let us consider once again eqs (1)–(3). Under the near field condition $\lambda z \ll d^2$ the propagator is a significantly local function which makes the region of small values of its argument in the integral to be preferential. In accordance with (3) the size of this region equals approximately $\Delta x_1 = \sqrt{\lambda z}$. For example, when $\lambda = 3 \cdot 10^{-9}$ cm ($E = 40$ keV), $z = 3$ cm one evaluates Δx_1 as 1 μm. Let us assume that the complex argument of the function $f_1(x)$ is smooth enough inside a region of this size. Then we can use the following approximate representation of the function $f_1(x)$ in the integral (2)

$$f_1(x_1) = \exp\{\xi(x_1)\},$$
$$\xi(x_1) \approx \xi(x) + \xi'(x)(x_1 - x) + \xi''(x)(x_1 - x)^2/2 \tag{10}$$

where

$$\xi = \alpha + i\phi, \qquad \xi' = \frac{d\xi}{dx}, \qquad \xi'' = \frac{d^2\xi}{dx^2}. \tag{11}$$

Substituting (10) in (2) and making a shift of variable of integration $x_1 - x = x_1' \to x_1$ one obtains instead of (2)

$$f_2(x) \approx (i\lambda z)^{-1/2} \int dx_1 \exp\left(\xi + \xi' x_1 + \frac{1}{2}\left(\xi'' + \frac{i}{\varepsilon}\right)x_1^2\right) \tag{12}$$

where $\varepsilon = \lambda z/2\pi$ is a small parameter. Here we assume that only one region inside the integral (2) is essential with $x_1 \approx x$ and the limits can remain infinite without loss of accuracy.

The integral (12) is calculated analytically with use of table integral [12]

$$\int dx \exp(\pm bx - cx^2) = \left(\frac{\pi}{c}\right)^{1/2} \exp\left(\frac{b^2}{4c}\right). \tag{13}$$

As a result we obtain

$$f_2(x) \approx (1 - i\varepsilon\xi'')^{-1/2} \exp\left(\xi + \frac{i\varepsilon}{2}\frac{\xi'^2}{(1 - i\varepsilon\xi'')}\right). \tag{14}$$

Let us represent $f_2(x)$ as

$$f_2(x) = \exp\{\eta(x)\}, \qquad \eta(x) = \beta + i\psi \tag{15}$$

and consider the value $\varepsilon\xi''$ to be small enough to use a power series expansion up to a second degree. As a result, we obtain the approximate local relation between η and derivatives of ξ in each point

$$\eta \approx \xi + \frac{i\varepsilon}{2}\xi'^2(1 + i\varepsilon\xi'') + \frac{i\varepsilon}{2}\xi'' - \frac{\varepsilon^2}{4}\xi''^2. \tag{16}$$

We are interested in the real part of this relation which represents a differential equation for the phase ϕ of the complex function $f_1(x)$. It is convenient to write this equation in terms of the variable $x_0 = \varepsilon\phi'$ in the following view convenient for the iterations

$$x_0' = \frac{2(\alpha - \beta) - \varepsilon^2(\alpha'^2\alpha'' + \frac{1}{2}\alpha''^2) - 2\alpha' x_0 + \alpha'' x_0^2 + \frac{1}{2}x_0'^2}{1 - 2\alpha' x_0}. \tag{17}$$

This is the main equation of the algorithm. The quantities α, α', α'', β are known from measurements, while x_0 is a value which we need to find for calculating the phase shift profile.

A practical implementation of the algorithm which I used in the calculations presented in the next section, is as follows. One chooses the width of the image region and introduces a set of points x_j, $j = 1, \ldots, N$ with a step d. The region may coincide with the measured data. Then one uses the approximate net values for the derivatives

$$\alpha_j' = \frac{\alpha_{j+1} - \alpha_{j-1}}{2d}, \qquad \alpha_j'' = \frac{\alpha_{j+1} + \alpha_{j-1} - 2\alpha_j}{d^2}. \tag{18}$$

At the beginning one may start with $x_{0j} = x'_{0j} = 0$ for all j and calculate a new value of x'_{0j} from eq. (17). Then one uses

the relations

$$x_{0j+1} = x_{0j} + \frac{d}{2}(x'_{0j} + x'_{0j+1})$$

$$\phi_{j+1} = \phi_j + \frac{d}{2\varepsilon}(x_{0j} + x_{0j+1}) \tag{19}$$

to obtain new values of x_{0j} and ϕ_j. The boundary conditions are naturally $x_{0j} = \phi_j = 0$ for $j = 1$. The self-consistent solution has to give the same for $j = N$ as well. However, it is very difficult to obtain the last limit values at each step of iteration. Moreover, owing to the fact that eq. (17) is approximate, these conditions may not be fulfilled even after a solution. To fulfil this one can use an artificial trick, namely, to redefine the calculated values x'_{0j} at each step of iteration by means of the relation

$$x'_{0j} \to x'_{0j} + C_1 x'^3_{0j} + C_2 x'^5_{0j} \tag{20}$$

where the coefficients C_1 and C_2 have to be found from the conditions $x_{0j} = \varphi_j = 0$ for $j = N$. It allows to include these conditions in the iterative procedure to improve the algorithm. Really, to find the coefficients C_1 and C_2 I searched the minimum of the functional $\Phi(C_1, C_2) = x^2_{0N} + \phi^2_N$ by means of multiple calculations of (19). New values of x_{0j} and x'_{0j} are used in eq. (17) once again and so on up to the moment when all values of the phase ϕ_j bcome unchanged within the chosen accuracy at the new step of iteration.

The convergence of the algorithm depends on the quality of data. Let us discuss this point in more detail. The approximation (12) to the integral (2) is valid when the equation for x_1

$$\frac{2\pi}{\lambda z}(x - x_1) + \phi'(x_1) = 0 \tag{21}$$

has only one solution with x as a parameter. In accordance with the stationary phase method [13] the solution of (21) gives just the point of stationary phase of the integrand. If the phase shift profile is smooth enough then indeed one solution only may exist at the point $x_1 \approx x$ because under the near field condition the value λz is small. The difference between the points x_1 and x just describes the inclination of a particular ray from the Z-axis owing to inhomogeneous phase distribution. However, real objects, for example fibers, contain regions near the boundary where this condition is not met. Indeed, for a round fiber the phase shift profile is as follows

$$\phi(x) = -\delta \frac{4\pi R}{\lambda} \sqrt{1 - \frac{x^2}{R^2}} \tag{22}$$

where δ is a decrement of the refractive index, R is the radius of the fiber. One can see that $\phi'(x)$ equals infinity at $x = \pm R$. This means that each fragment of the complex object having such a structure, will incline the rays in the outer part at arbitrary angles. As a result, we obtain two or more solutions of (21) in some regions of the hologram. The existence of several stationary phase points gives a rise of fast oscillations of intensity thanks to the interference between the good ray which is inclined at small angle and several bad rays of small amplitude which are inclined at large angles. These oscillations are clearly seen in a computer simulation with a completely coherent incident wave (see the next Section). However these can only be partially recorded in an experiment owing to a partial loss of coherence.

It is clear that fast oscillations of small amplitude are undesirable for both the experiment and the method presented. The latter supposes a single-valued correspondence between the rays leaving the first hologram plane and those entering the second hologram plane. That is why before an application of the method the measured data have to be smoothed by averaging over a region of size $2\sqrt{\lambda z}$ or more. This allows to provide the convergence of the procedure by means of both eliminating the numerical difficulties and the elimination of undesirable interference between good ray and bad rays. As a result, the derivative of the phase shift becomes smoothed which leads to a smoothed phase shift profile. Therefore small details of the phase shift profile may disappear while the main details are reconstructed well as it is demonstrated in the next Section.

4. Computer simulation

The main application of the phase retrieval method is hard X-ray refraction tomography. That is why I have considered for a computer simulation the object shown in Fig. 1, namely, a complex of four fibers of different matter: boron with a tungsten core, aluminum and silicon. The fibers have different radii and position. The energy of the X-rays is $E = 50\,\text{keV}$ ($\lambda = 0.248\,\text{Å}$). It is convenient to make one measurement of intensity just after the object. In this case the function $f_1(x)$ really has the form of an exponential function

$$f_1(x) = \exp\{\xi(x)\},$$

$$\xi(x) = -\frac{4\pi}{\lambda} \sum_{j=1}^{4} R_j(\beta_j + i\delta_j) \sqrt{1 - \frac{(x - x_j)^2}{R_j^2}} \tag{23}$$

where the square root of the negative argument is assumed to be zero, β_j is the index of absorption, δ_j is the decrement of the refractive index, R_j is the radius and x_j is the position of the j-th fiber. These parameters are shown in Table I. The δ value for W is given after subtraction of the B value. As it follows from Table I, tungsten only is able to absorb X-rays while all other materials are practically transparent. This is clearly seen in Fig. 1 where the intensity profile just after the object is shown as a first hologram.

The object considered is out of the applicability of the method in a pure sense (see above) because the function $\xi(x)$ is not a smooth function near the boundary. So, in order to verify the method in a pure sense let us consider, first of all, the results for a smoothed profile $\overline{\xi(x)}$ which was obtained from $\xi(x)$ (23) by convolution with a Gaussian of 20 μm half-width. The holograms of this artificial object at zero distance and $z_2 = 20\,\text{cm}$ are shown in Fig. 2. Both intensities have a unit background and a second curve is shifted vertically by 0.2 to have a better view. The second curve differs

Table I. *Parameter values for computer simulations*

j	M	R (μm)	x (μm)	$\beta \cdot 10^7$	$\delta \cdot 10^7$
1	B	30	−20	0.00002	1.79
2	W	10	−20	0.198	10.7
3	Al	20	30	0.00091	2.14
4	Si	0	12	0.00107	1.91

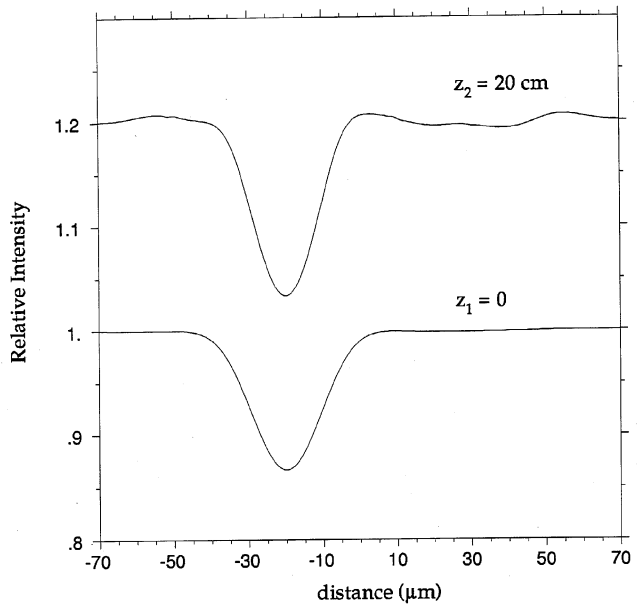

Fig. 2. Relative intensity distribution in two holograms for a smoothed object.

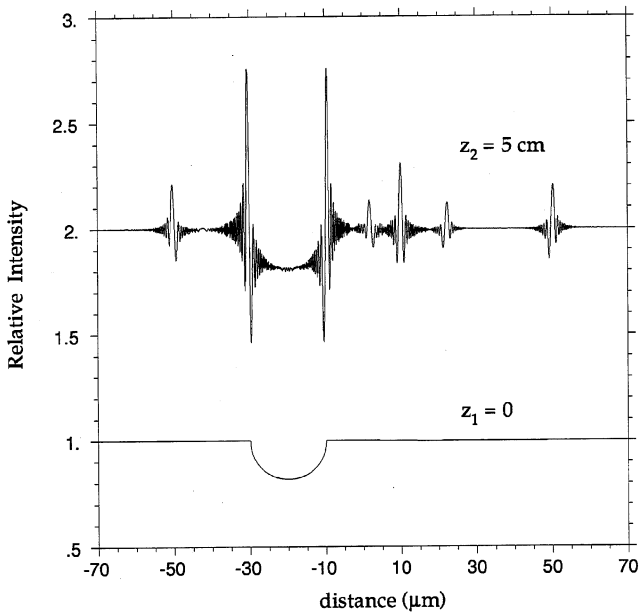

Fig. 4. Relative intensity distribution in two holograms for a real object.

only slightly from the first one and both curves are smooth enough. A direct application of the method allows to reconstruct fastly the phase shift profile for the object. No additional smoothing is necessary. The result is shown in Fig. 3 where the thin curve is an original phase shift curve while the thick curve is a reconstructed curve. One can see that the difference in contrast is very weak and there may arise experimental difficulties to record this small difference. However, I suppose that the difference can be measured accurately and consider small z especially to demonstrate the possibility to work under the near-field condition. Naturally, for this smooth object the method works for longer distances as well with a better contrast.

Holograms for a real object are shown in Fig. 4. The second curve is shifted by 1 vertically. Thanks to the abrupt boundaries a strong contrast and strong interference fringes arise even at a distance $z_2 = 5$ cm. The data of Fig. 4 as well as all other data were calculated with a step 0.1 μm. Naturally, it is impossible to use the data of Fig. 4 in the method proposed and it is very difficult to measure the fringe pattern because the resolution of the modern detectors (the nuclear films) does not exceed 1 μm. To eliminate the undesirable interference fringes one can make the procedure of smoothing. It occurs just in an experiment under the conditions of partial loss of coherence and finite detector resolution. Fig. 5 shows the result of smoothing the data by means of a Gaussian with a half-width of 2 μm. Here the vertical shift is 0.5. It is clearly seen that the interference fringes disappear while the contrast is good enough to record. The result of the application of the method to these data is shown in Fig. 6. One can see that there is a correspondence between the original phase shift profile (thin curve) and the reconstructed profile (thick curve). Thus, the method can be used for such objects as well. The advantage of this technique is the fact that a loss of coherence and a

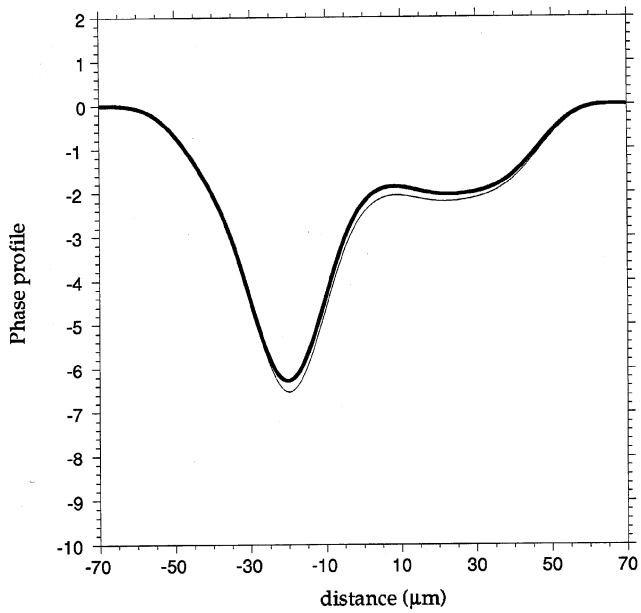

Fig. 3. Original (thin curve) and reconstructed (thick curve) phase shift profiles for a smoothed object.

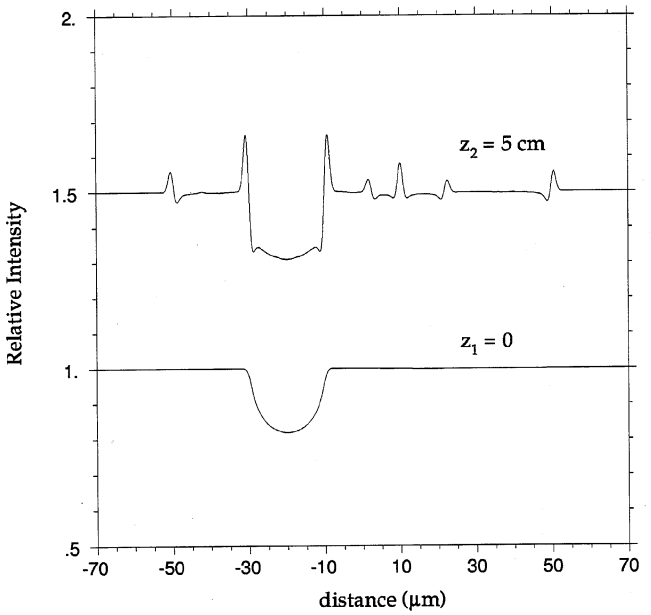

Fig. 5. The curves of Fig. 4 smoothed by a Gaussian of 2 μm halfwidth.

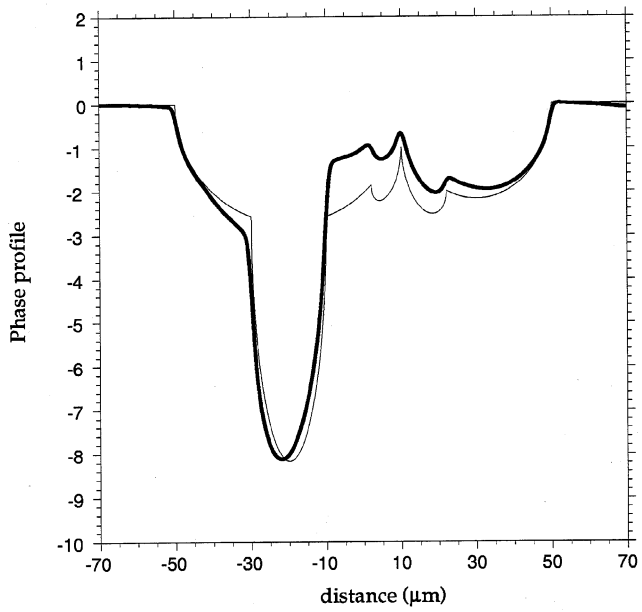

Fig. 6. Original (thin curve) and reconstructed (thick curve) phase shift profiles from data of Fig. 5.

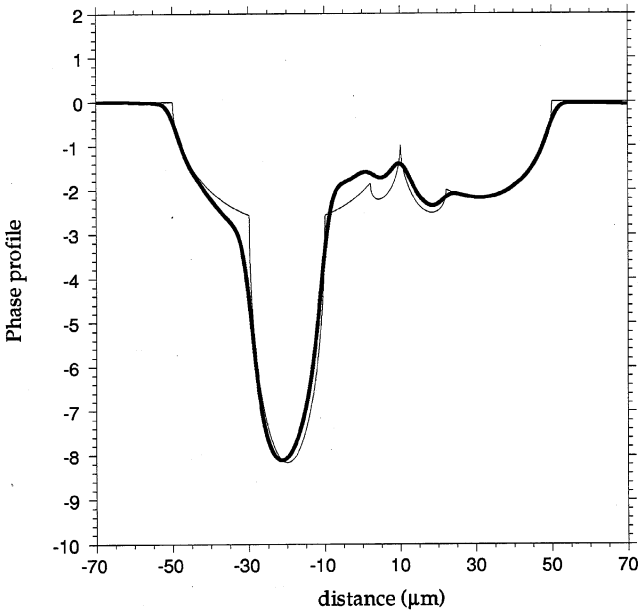

Fig. 8. Original (thin curve) and reconstructed (thick curve) phase shift profiles from data of Fig. 7.

bad detector resolution are preferential. Therefore this method is a find for poor experimentators.

Let us discuss the reason for the small difference between original and reconstructed curves. The maximum difference arises in the central part near the tungsten boundary. It is owing to the fact that smoothing can kill the interference fringes between a good ray (slightly inclined) and bad rays (significantly inclined) but cannot kill the intensity itself of these bad rays which still exists in the contrast at one place and is absent in another place. This intensity is not taken into account in eq. (17). Therefore the second derivative of the phase shift becomes overestimated or underestimated in different points. I shall try to find a way to take this fact into account in a future work to improve the method. However, today I don't see how to do this. It is of interest that a more rough smoothing leads to a worse contrast but gives a better result for a reconstruction. This is demonstrated in Figs. 7 and 8 where the same calculation was performed after a smoothing over 5 μm. Despite the fact that abrupt boundaries are not reconstructed, the average correspondence becomes better.

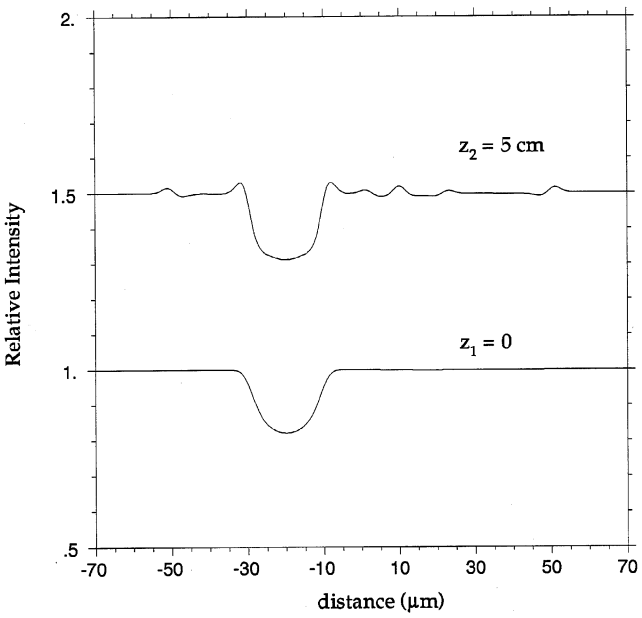

Fig. 7. The curves of Fig. 4 smoothed by a Gaussian of 5 μm halfwidth.

Acknowledgements

The author would like to thank Dr. A. Snigirev, Dr. I. Snigireva and C. Raven for helpful discussions.

References

1. Gabor, D., Proc. Roy. Soc. **A197**, 454 (1949); Proc. Phys. Phys. Soc. (London) **B64**, 449 (1951).
2. Baez, A. V., J. Opt. Soc. Amer. **42**, 756 (1952).
3. Tyler, G. A. and Tomson, B. J., Opt. Acta **23**, 685 (1976).
4. Onural, L. and Scott, P. D., Opt. Eng. **26**, 1124 (1987).
5. Koren, G., Polack, F. and Joyeux, D., J. Opt. Soc. Amer. **A10**, 423 (1993).
6. Nugent, K. A., Opt. Commun., **78**, 293 (1990).
7. Maleki, M. H. and Devaney, J., Opt. Eng. **33**, 3243 (1994).
8. Snigirev, A., Snigireva, I., Kohn, V., Kuznetsov, S. and Schelokov, I., Rev. Sci. Instrum. **66**, 5486 (1995).
9. Raven, C. *et al.*, Appl. Phys. Lett. **69**, 1826 (1996).
10. Gerchberg, R. W., Saxton, W. O., Optik **35**, 237 (1972).
11. Fienup, J. R., Appl. Opt., **21**, 2758 (1982).
12. Cowley, J. "Diffraction Physics" (North-Holland, Amsterdam 1975).
13. Jeffreys, H. and Swirles, B. "Methods of Mathematical Physics," (Cambridge, 1966).